Diagn Interv Radiol 2013; 19:438–446

CHEST IMAGING
ORIGINAL ARTICLE

Clinical and radiologic manifestations of pulmonary cryptococcosis in immunocompetent patients and their outcomes after treatment

Thitiporn Suwatanapongched, Wasinan Sangsatra, Viboon Boonsarngsuk, Siriorn P. Watcharananan, Pimpin Incharoen

PURPOSE
We aimed to investigate clinical and radiologic manifestations of pulmonary cryptococcosis in immunocompetent patients and their outcomes after treatment.

MATERIALS AND METHODS
We retrospectively reviewed the medical records, initial and follow-up chest computed tomography scans and/or radiographs for initial clinical and radiologic manifestations and outcomes following antifungal treatment of 12 immunocompetent patients diagnosed with pulmonary cryptococcosis between 1990 and 2012.

RESULTS
Twelve patients (age range, 21–62 years; males, eight patients [66.7%]) were included. Nine (75%) patients were symptomatic, eight of whom had disseminated infection with central nervous system involvement. Initial pulmonary abnormalities consisted of single nodules/masses (n=5), single segmental or lobar mass-like consolidation (n=3), multiple cavitary and noncavitary nodules (n=1), and multifocal consolidation plus nodules (n=3). These lesions ranged from less than 1 cm to 15 cm in greatest diameter. Distinct subpleural and lower lung predominance was observed. Seven patients (58.3%) had one or more atypical/aggressive findings, namely endobronchial obstruction (n=4), calcified (n=1) or enlarged (n=4) mediastinal/hilar lymph nodes, vascular compression (n=1), pericardial involvement (n=1), and pleural involvement (n=2). Following antifungal therapy, radiologic resolution was variable within the first six months of eight nonsurgical cases. Substantial (>75%) improvement with some residual abnormalities, bronchiectasis, cavitation, and/or fibrotic changes were frequently observed after 12–24 months of treatment (n=6).

CONCLUSION
Pulmonary cryptococcosis in immunocompetent patients frequently causes disseminated infection with atypical/aggressive radiologic findings that are gradually and/or incompletely resolved after treatment. The presence of nonenhanced low-attenuation areas within subpleural consolidation or mass and the absence of tree-in-bud appearance should raise concern for pulmonary cryptococcosis, particularly in patients presenting with meningitis.

From the Departments of Radiology (T.S. ✉ *ratrspoom@yahoo.com*, W.S.), Pulmonary and Critical Care Medicine (V.B.), Infectious Diseases (S.P.W.), and Pathology (P.I.), Ramathibodi Hospital, Mahidol University Faculty of Medicine, Bangkok, Thailand; Banmi Hospital (W.S.), Lopburi Province, Thailand.

Received 13 February 2013; revision requested 9 March 2013; revision received 2 April 2013; accepted 10 April 2013.

Published online 18 July 2013.
DOI 10.5152/dir.2013.13049

Pulmonary cryptococcosis is an emerging infection caused by *Cryptococcus* species complex, which are ubiquitous encapsulated yeasts found worldwide. The infection usually affects immunocompromised patients, particularly those with an impaired cell-mediated immune response (1, 2). In rare circumstances, the infection occurs in otherwise healthy individuals. According to previous studies from many countries in North America, Europe, and the East (3–11), most immunocompetent individuals have mild or no clinical symptoms with isolated pulmonary involvement through single or multiple small pulmonary nodules. These findings are somewhat different from the more aggressive clinical and radiographic findings described in isolated case reports among Thai immunocompetent patients (6, 12–14) and in a study from South America (3). Therefore, there might be potential differences in the clinical and radiologic characteristics of pulmonary cryptococcosis among different geographic regions and hospital settings. Although radiologic responses to treatment have been previously mentioned (3–6, 9–11), specific details regarding the radiologic changes in pulmonary cryptococcosis following antifungal therapy are still limited and are usually based on follow-up chest radiographs. This information led us to ascertain clinical and radiologic manifestations of pulmonary cryptococcosis among Thai immunocompetent patients and their outcomes following antifungal therapy.

Materials and methods

Study population

This retrospective study was approved by the Local Ethics Committee on Human Rights related to research involving human subjects at our institution. Patient consent was waived because the investigations and management were part of routine patient care, and patient confidentiality was strictly maintained by our methods.

We retrospectively searched our hospital database between 1990 and 2012 for adult patients (aged ≥18 years) who had evidence of cryptococcal infection and/or positive cryptococcal antigen (CRAG) tests in serum or cerebrospinal fluid (CSF). Patients with coexisting human immunodeficiency virus or other immunocompromised diseases (i.e., hematologic or solid organ malignancies, kidney transplantation, collagen vascular disease, diabetes mellitus, liver cirrhosis, and immunosuppressive therapy) or unavailable medical records were excluded. The criteria used for the diagnosis of pulmonary cryp-

tococcosis included the histopathological presence of the organism in a resected lung specimen or from a lung biopsy, a positive culture of a respiratory specimen for *Cryptococcus spp.,* or a positive serum CRAG test, regardless of titer value, with clinical or radiographic evidence of active pulmonary disease. Disseminated infection was considered when there was an evidence of extrathoracic involvement—i.e., positive CSF culture for *Cryptococcus spp.,* positive CSF CRAG test, or clinical or radiologic evidence of other organ involvement in addition to pulmonary disease.

During the study period, 24 apparently immunocompetent patients had documented cryptococcal infection. We further excluded 12 patients who did not meet our criteria for the diagnosis of pulmonary cryptococcosis, leaving 12 patients for analysis. The patients' medical records were retrospectively reviewed for their demographics (age, gender, occupation, tobacco smoking status, and exposure to pigeon droppings or eucalyptus trees), clinical presenting symptoms (fever, headache, cough, sputum production, hemoptysis, weight loss, and night sweats), treatments (types and dosage of antifungal drugs and surgical intervention), clinical response and outcomes after antifungal treatment.

Laboratory data, including CRAG titers in serum and CSF; India ink-stained preparation; culture and/or molecular identification for *Cryptococcus spp.* from bronchoalveolar lavage fluid, blood, and CSF; and/or histopathology results of biopsy specimens (lung, lymph node, and skin), were also reviewed.

Radiologic assessment

All chest computed tomography (CT) and chest radiographs of these patients were retrospectively reviewed by two observers, and the results were reached by consensus. Both nonenhanced and contrast-enhanced chest CT scans were obtained in most patients. The CT scans were performed using various scanners, including an electron-beam CT scanner (Imatron, San Francisco, California, USA), as well as 4-slice (LightSpeed plus, General Electric Medical Systems, Milwaukee, Wisconsin, USA), 16-slice (Mx8000 IDT, Philips, Eindhoven, The Netherland), and 64-slice (Sensation Cardiac 64, Siemens Healthcare, Erlangen/Muenchen, Germany) multidetector CT scanners. The CT parameters (120 kVp, 80–220 mAs) and the slice thickness (2–10 mm) used were variable depending on the type of the CT scanner. All CT images were reconstructed with standard and high-spatial frequency algorithms for mediastinal- and lung-window displays, respectively.

Initial pulmonary parenchymal abnormalities were classified as a pulmonary nodule or mass (a rounded or oval-shaped opacity ≤3 cm or >3 cm in diameter, respectively), airspace consolidation (a nonrounded, subsegmental, segmental, or lobar opacity obscuring the underlying vascular structures), groundglass opacity (opacity without obscuration of the underlying vascular structures), miliary pattern, and centrilobular branching or tree-in-bud appearance.

The number and greatest dimension of the pulmonary nodules, masses, and consolidation were determined. The location of the abnormalities was defined based on the pulmonary lobes and zonal involvement (peripheral, subpleural or pleural-based, middle 1/3, or perihilar). The margins of the nodules/masses were classified as well- or ill-defined with a smooth, lobulated, irregular or spiculated border. The presence of air- or mucus-filled bronchograms, cavitation, calcification, the pattern of contrast enhancement (homogeneous or heterogeneous), the presence of enhancing vessels (the so-called CT angiogram sign) and nonenhanced low-attenuation areas within the masses or consolidated areas were determined whenever possible. Associated airway abnormalities (bronchial wall thickening, bronchiectasis, endobronchial obstruction) were assessed as present or absent.

Mediastinal or hilar lymphadenopathy (lymph node with a short axis diameter ≥10 mm), nodal calcification, pleural abnormalities (effusion, thickening, and calcification), cardiovascular abnormalities (pericardial effusion, vascular encasement/compression), and upper abdominal organ involvement were assessed.

Radiologic changes and/or outcomes after antifungal therapy were determined based on follow-up chest CT or chest radiographs <1 month, 1–3 months, >3–6 months, >6–12 months, >12–24 months, and >24 months after initiation of antifungal therapy. If more than one imaging modality were available, the latest CT or chest radiograph (when CT was unavailable) obtained in each period was used for analysis. In each patient, the improvement of parenchymal abnormalities was visually estimated by comparing the sizes and/or numbers of the pulmonary nodules, masses and/or consolidations with those observed on the initial imaging using a five-point scale as follows: 0, no improvement; 1, improved <25%; 2, improved 25%–50%; 3, improved >50%–75%; and 4, improved >75%. Resolution of extrapulmonary abnormalities, including re-establishment of airway and superior vena cava patency, as well as associated cavitation, cyst formation, calcification, air bronchogram, bronchiectasis, and fibrotic change (the presence of architectural distortion and a parenchymal scar) were also determined from CT.

Results

Clinical manifestations and pathological findings

Eight (66.7%) of the 12 patients were men. The patients' median age was 51 years (range, 21–62 years). Six patients worked in agricultural fields of rice or fruits, and two were construction laborers. Four patients had an exposure to pigeon excreta. Three of the male patients were

current smokers, and one was a former smoker. Nine patients (75%) were symptomatic. The common presenting clinical symptoms included headache (n=5), fever (n=4), and chronic cough (n=4). The median onset of clinical illness was 2.5 months (range, 0.5–8 months) prior to presentation.

Cryptococcomas (fibrogranulomatous nodules with multinucleated giant cells and numerous yeasts) were found in the surgical specimens of two patients. Pathological examination of the lung biopsy specimens (Fig. 1) revealed histiocyte aggregations or poorly formed granulomas with numerous yeasts within histiocytes and minimal inflammatory response (n=5) and coexisting fibrosis (n=3). Sputum (n=3), bronchoalveolar lavage fluid (n=2), and/or CSF (n=7) cultures yielded *C. neoformans var. grubii* (serotype A) in seven patients (58.3%). Cultures were unavailable in the remaining patients.

As shown in Table 1, eight patients (66.7%) had disseminated infection to the central nervous system (CNS), including cryptococcal meningitis (n=8), and cranial nerve (n=1) and cerebral (n=1) involvement. Cutaneous (n=1) and probable splenic (n=1) involvement were also observed.

Initial radiologic manifestations

As shown in Table 1, initial radiologic abnormalities were determined based on chest CT findings in eight patients and chest radiographic findings in four patients (no. 1–4). The median interval between initial chest radiographs or initial chest CT and definitive diagnosis was 12 days (range, 3–66 days). Nine (75%) of the 12 patients had unilobar involvement of a single pulmonary nodule/mass (n=5, Fig. 1), a single segmental or lobar mass-like consolidation (n=3, Figs. 2, 3), or a cluster of cavitary and noncavitary pulmonary nodules (n=1). The remaining three patients (25%) had multilobar involvement by multiple subsegmental/segmental areas of consolidation plus small nodules (Fig. 4). Distinct peripheral, subpleural, or pleural-based involvement was observed with all single lesions and most multiple lesions. The lower lung zones were involved in 11 patients (91.6%), and the right middle lobe was involved in seven patients (58.3%). These lesions ranged from <1 cm up to 15 cm in greatest diameter. All of the single pulmonary nodules/masses and most of the multiple pulmonary nodules/masses were solid in appearance and had a rather well-defined but slightly lobulated or irregular mar-

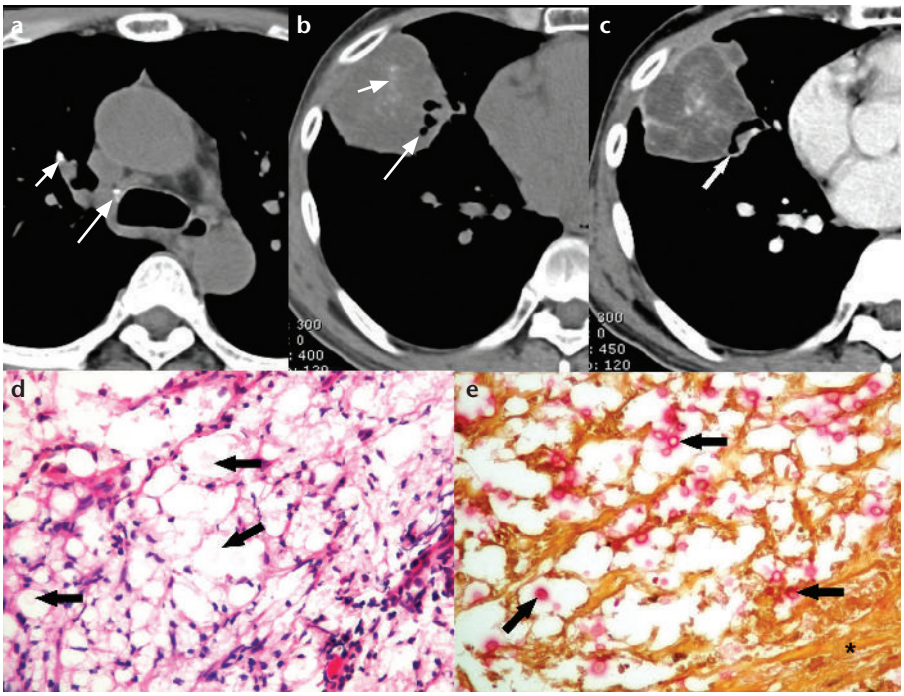

Figure 1. a–e. A 51-year-old man (patient no. 9) with a large cryptococcoma. Axial nonenhanced **(a, b)** and contrast-enhanced **(c)** CT scans at initial presentation show a small calcified peribronchial node in the right upper lobe **(a,** *short arrow)*, a partially calcified right lower paratracheal node **(a,** *long arrow*), a large pleural-based mass at the right middle lobe containing irregular foci of central calcifications **(b,** *short arrow)*, and multiple nonenhanced low-attenuation areas **(c)**. Complete endobronchial obstruction and mild dilatation of the proximal air-filled bronchi **(b, c,** *long arrows)* are noted. Hematoxylin and eosin staining (×40, **d**) and mucicarmine staining (×40, **e**) of the transthoracic needle biopsy specimen of the right middle lobe mass reveal histiocyte aggregations or poorly formed granulomas with numerous intracytoplasmic yeasts and thick pink capsules **(d, e,** *arrows)* and areas of loose fibrosis **(e,** *asterisk*), corresponding to the nonenhanced low-attenuation areas within the mass demonstrated on CT.

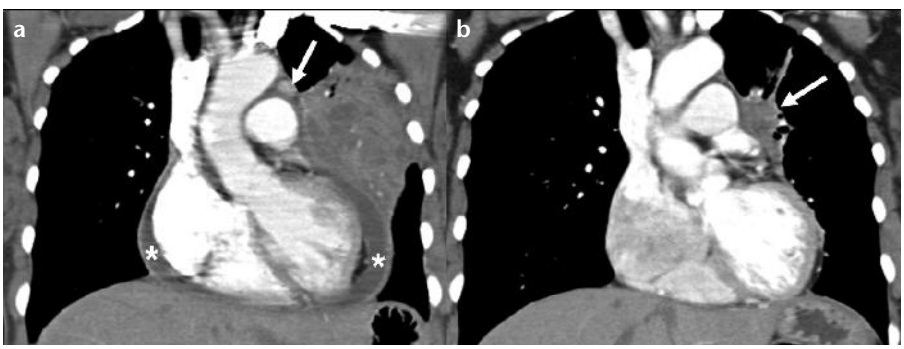

Figure 2. a, b. A 48-year-old woman (patient no. 10) with pulmonary and pericardial cryptococcosis. Coronal contrast-enhanced CT scan **(a)** at initial presentation shows a large, heterogeneously enhancing area of consolidation with several low-attenuation areas involving the superior and inferior lingula. Diffuse pericardial thickening with pericardial effusion (*asterisks*) and an enlarged aortopulmonary window node *(arrow)* are observed. After 15 months of antifungal therapy, follow-up CT **(b)** shows a marked decrease in the size of the consolidated area with a small residual mass-like lesion *(arrow)* at the affected region. Note the complete interval resolution of pericardial thickening, pericardial effusion, and the enlarged node.

Table 1. Summary of initial clinical and radiologic manifestations of 12 patients with pulmonary cryptococcosis

Patient no. (Age [years]/ gender)	Year	Clinical findings			Radiologic findings										
								Dominant parenchymal abnormalities		Associated findings in the pulmonary lesion			Additional CT findings		
		Clinical presentation	Disseminated infection with CNS involvement	Initial serum/CSF CRAG test or titers	Imaging modality	Site of lesion(s)	Mode of biopsy (site)	Nodules /masses (size [cm])	Consolidated area (size [cm])	LAA	Cavity	AB	EBO	LN	Others
1 (41/F)	1990	headache,	+	1:64/1:64	CXR	RLL	surgery (lung)	single (3.3)	-	-	-	-	NA	NA	NA
2 (21/M)	1990	headache	+	1:4/1:16	CXR	RML	NA	single (3.5)	-	-	-	-	NA	NA	NA
3 (33/M)	1997	headache, hearing loss, weakness, ataxia	+	1:1024/ 1:512	CXR	RML	NA	single (2.5)	-	-	-	+	NA	NA	NA
4 (59/M)	1998	chronic cough	+	1:128/1:32	CXR	LLL	TBBX[a]	multiple (1.0–2.5)	-	-	+	-	NA	NA	NA
5 (51/F)	2002	asymptomatic	+	1:1024/ 1:128	CT	RLL	TBBX (lung)	-	single (7.4)	+	-	-	+	-	splenic nodules
6 (53/M)	2003	chronic cough	+	+ve/1:128	CT	all	TBBX (lung)	multiple (0.3–2.0)	multiple (12.5)	+	+	+	-	+[b]	minimal pleural effusion and thickening
7 (62/M)	2007	chronic cough, fever, weight loss	-	+ve/-ve	CT	RUL, RML, RLL, LLL	TTNA[a], TBBX[a] (lung)	multiple (0.2–2.0)	multiple (3.5–5.4)	-	+	+	-	+[b]	-
8 (58/F)	2007	fever, weight loss	-	+ve/-ve	CT	RML	TBBX (LN)	-	single (15.0)	+	-	-	+	+[b]	vascular compression
9 (51/M)	2008	headache, fever, ataxia, blurred visions	+	>1:1024/ 1:1024	CT	RML	TTNB (lung, skin)	single (8.0)	-	+	-	+	+	-	calcified LN, calcified nodules in liver and small bowel, left eyelid and intracerebral nodules
10 (48/F)	2009	headache, chronic cough, hemoptysis, fever, pleuritic chest pain, weight loss	+	1:1024/ 1:512	CT	lingula	TTNB (lung)	-	single (7.8)	+	-	-	+	+[b]	pericardial effusion and thickening
11 (40/M)	2010	asymptomatic	-	1:128/-ve	CT	RML, RLL	TBBX (lung)	multiple (0.2–0.9)	multiple (1.0–3.0)	-	-	+	-	+	minimal pleural effusion, calcified nodules
12 (54/M)	2012	asymptomatic	-	-ve/-ve	CT	LLL	surgery (lung)	single (2.0)	-	-	-	+	-	-	-

[a]nondiagnostic result, [b]≥10 mm in short axis diameter.
AB, air bronchograms; CNS, central nervous system; CRAG, cryptococcal antigen; CSF, cerebrospinal fluid; CT, computed tomography; CXR, chest radiograph; EBO, endobronchial obstruction; F, female; LAA, low-attenuation areas; LLL, left lower lobe; LN, lymph node; M, male; NA, not available; RLL, right lower lobe; RML, right middle lobe; RUL, right upper lobe; TBBX, transbronchial biopsy; TTNA, transthoracic needle aspiration; TTNB, transthoracic needle biopsy; + , present; -, absent; +ve, positive CRAG titer but not quantified; -ve , negative CRAG titer.

gin. Air bronchograms and/or small air-filled cavities within the nodules/ masses were frequently visible on CT in seven cases (58.3%). Flecks of calcification within the pulmonary mass were observed in one case (Fig. 1a, 1b). Multiple small, calcified nodules were found in one case. Surrounding groundglass opacity, the so-called CT halo sign, was evident in two patients (Fig. 4a). No fibrotic change, bronchiectasis, isolated groundglass opacity, miliary pattern, or tree-in-bud appearance was observed.

Following intravenous contrast enhancement, most nodules larger than 1 cm showed mild but homogeneous contrast enhancement, whereas all large masses or consolidated areas exhibited heterogeneous enhancement in association with a CT angiogram sign, nonenhanced low-attenuation areas and/or mucus-filled bronchograms (Figs. 1c, 2a, 3b). Obstruction of the segmental or lobar bronchi within the pulmonary mass or the area of postobstructive pneumonitis was also evident in four patients (33.3%) (Figs. 1b, 1c, 3b).

Six (50%) of the 12 patients had at least one extrapulmonary CT finding, consisting of calcified lymph nodes (n=1, Fig. 1a, 1b), enlarged mediastinal/hilar lymph nodes ranging from 10 to 38 mm in short axis diameter (n=4, Figs. 2a, 3a), compression of the superior vena cava and distal right pulmonary artery (n=1, Fig. 3a), and involvement of the pericardium (n=1, Fig. 2a), pleura (n=2), and extrathoracic organs (n=2).

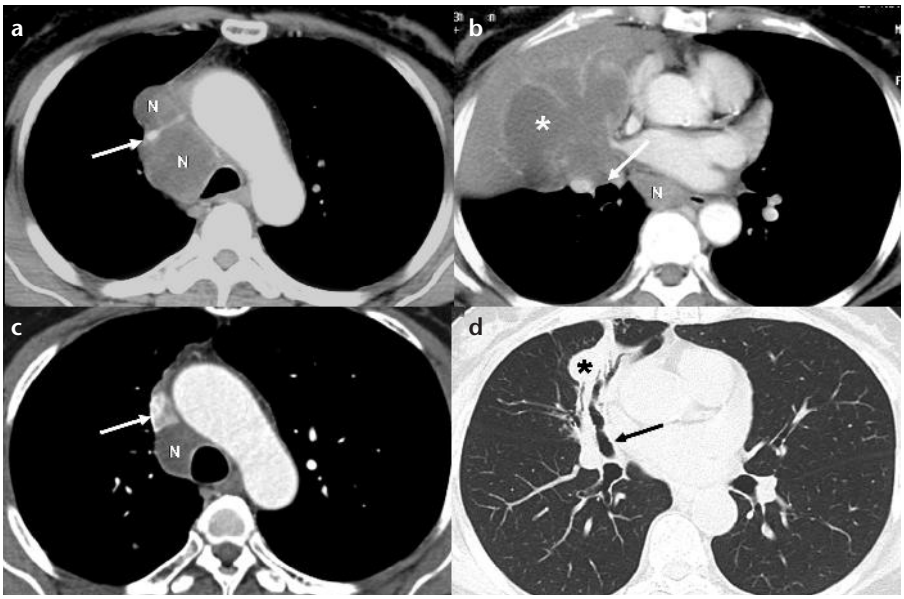

Figure 3. a–d. A 58-year-old woman (patient no. 8) with pulmonary cryptococcosis and lymphadenopathy. Axial contrast-enhanced CT scans **(a, b)** at initial presentation show a large central mass (**b,** *asterisk)* with complete obstruction at the origin of the right middle lobe bronchus (**b,** *arrow),* resulting in postobstructive pneumonitis in the remaining right middle lobe. Markedly enlarged nodes (N) at the right lower paratracheal and prevascular regions, compressing the superior vena cava (**a,** *arrow),* are observed. After 26 months of antifungal therapy, follow-up CT scans **(c, d)** show a substantial decrease in the size of the right middle lobe mass and enlarged nodes with complete resolution of postobstructive pneumonitis and reestablishment of the airway **(d,** *arrow)* and the superior vena cava (**c,** *arrow)* lumens. Note a residual nodule (**d,** *asterisk)* and bronchiectatic changes within the affected region.

Clinical and radiologic outcomes after treatment

Two patients (no. 1 and 12) underwent lobectomy because of uncertainty in the clinical diagnosis and had no radiographic evidence of recurrence after surgery. Ten patients (no. 1–10) required induction with intravenous amphotericin B, and six of them subsequently received oral fluconazole. Two patients (no. 9 and 12) received only oral fluconazole. The duration of oral fluconazole in eight patients ranged from 4–52 months (median, 33 months).

Because of obstructive hydrocephalus, two patients (no. 1 and 3) required ventriculoperitoneal shunts. Patient no. 3 also had permanent hearing loss and visual impairment. Patient no. 6 with extensive pulmonary cryptococcosis developed respiratory failure shortly after admission and required mechanical ventilation for two months. The patient subsequently improved but eventually required home oxygen therapy. Other symptomatic patients had clin-

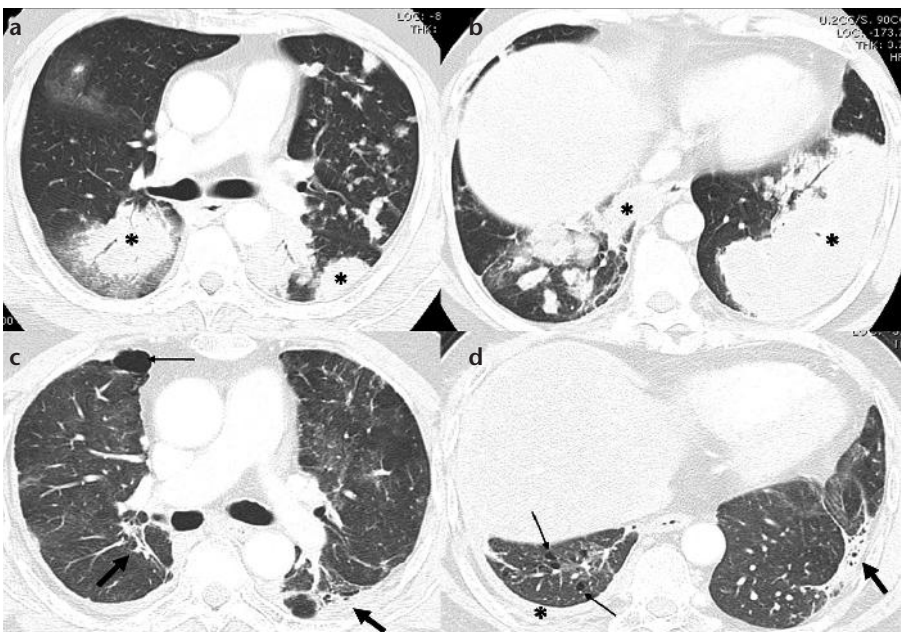

Figure 4. a–d. A 53-year-old man (patient no. 6) with extensive pulmonary cryptococcosis. Axial contrast-enhanced CT scans **(a, b)** at initial presentation show multiple small nodules and multifocal areas of peripheral or pleural-based consolidation *(asterisks)* in both lungs. Surrounding groundglass opacity, the so-called CT halo sign, around the consolidated area in the right lung is clearly demonstrated. After 50 months of antifungal therapy, follow-up CT scans **(c, d)** show complete interval resolution of the previous nodules and consolidations, leaving residual parenchymal fibroses and associated traction bronchiectasis/bronchiolectasis *(thick arrows).* Additionally, note the diffuse groundglass opacities in the remaining lung parenchyma, thin-walled subpleural cysts *(thin arrows),* and a smooth rind of pleural thickening on the right (**d,** *asterisk).*

Table 2. Summary of radiologic outcomes of pulmonary cryptococcosis after antifungal therapy in eight nonsurgical patients, using a 5-point scale

Patient no. (Age [years]/ gender)	Follow-up imaging	Scores of radiographic improvement and associated changes following antifungal therapy					
		<1 month	1–3 months	>3–6 months	>6–12 months	>12–24 months	>24 months
3 (33/M)	CT	0	NA	NA	NA	NA	NA
4 (59/M)	CXR	1 (cavitation)	NA	NA	NA	NA	NA
6 (53/M)	CXR/CT	NA	NA	NA	NA	4 (cavitation, bronchiectasis, fibrosis)	4 (cavitation, bronchiectasis, fibrosis)
7 (62/M)	CXR/CT	3	NA	4 (cavitation, fibrosis)	4 (cavitation, fibrosis)	4 (cavitation, fibrosis)	4 (cavitation, fibrosis)
8 (58/F)	CXR/CT	2	3 (cavitation, bronchiectasis)	3 (bronchiectasis, fibrosis)	4 (bronchiectasis, fibrosis)	4 (bronchiectasis, fibrosis)	4 (bronchiectasis, fibrosis)
9 (51/M)	CXR	1	NA	2	3 (fibrosis)	4 (fibrosis)	NA
10 (48/F)	CXR/CT	1	NA	2 (cavitation)	3	4 (bronchiectasis, fibrosis)	4 (bronchiectasis, fibrosis)
11 (40/M)	CXR/CT	NA	1 (fibrosis)	1 (fibrosis)	2 (fibrosis)	3 (fibrosis)	3 (fibrosis)

CT, computed tomography; CXR, chest radiograph; F, female; M, male; NA, not available.
5-point scale: 0, no improvement, 1, improved <25%; 2, improved 25%–50%; 3, improved >50%–75%; 4, improved >75%.

ical improvement within a month of treatment. All patients remained alive at the time of hospital discharge (n=2) or their last visit (n=9), ranging from two months to 107 months (median, 42 months).

Eight of the remaining patients had available follow-up chest CT scans and/or chest radiographs, with a range of 0.5–100 months (median, 29 months) after antifungal treatment. Based on available chest CT and/or chest radiographs in each period, radiologic resolution following antifungal therapy was variable within the first six months (Table 2). Half of the cases showed slight improvement (≤50%) of parenchymal abnormalities, including endobronchial obstruction and postobstructive pneumonitis, within one month of treatment. Further but gradual improvement along with interval development of air bronchograms and/or bronchiectatic changes (n=4), cavitation (n=4), and/or fibrotic changes (n=5) in the resolving lesions was usually observed thereafter.

Notably, one patient (no. 8) developed a small cavity, groundglass opacity, and tree-in-bud appearance at the right upper lobe four months after antifungal treatment. The lesions subsequently proved to be due to coexisting tuberculosis. After dual treatment with antifungal and antituberculous drugs, there was partial resolution of both pulmonary tuberculosis and cryptococcosis along with gradual reduction in nodal sizes (Fig. 3c, 3d).

In six patients, substantial improvement (>75%) along with complete resolution of pericardial (Fig. 2b) and pleural involvement were evident after 12 months of treatment. However, all of them had some residual pulmonary parenchymal and/or nodal abnormalities, as well as fibrotic and/or bronchiectatic changes in the affected regions after 24 months of treatment. As shown in Fig. 4c, 4d, there was subsequent development of several subpleural and/or intraparenchymal cysts in the right lung, diffuse groundglass opacity in the remaining lung parenchyma, smooth right pleural thickening, and interval calcifications of bilateral lower paratracheal nodes in one patient (no. 6).

Discussion

To the best of our knowledge, our study is the first original study describing pulmonary cryptococcosis among immunocompetent patients in Southeast Asia. As shown in our study, our patients had a wider range of clinical and radiologic manifestations, ranging from asymptomatic colonization to disseminated infection than those reported previously. In contrast to the previous studies from other countries in which most cases were asymptomatic and had isolated or limited pulmonary involvement (3–6, 8–11), most of our patients had either symptomatic or disseminated infection with more aggressive and/or atypical radiologic manifestations at the initial presentation. Although most of our patients also had unilobar pulmonary involvement, a finding that was different from previous studies showing multiple lesions, multilobar, or bilateral pulmonary involvement (5–10), and the sizes of the pulmonary nodules, masses and/or consolidations in our patients were more variable, ranging from <1 cm up to 15 cm in greatest diameter. The distinct peripheral, subpleural, and lower lung predominance in the present study was similar only to the findings reported by Fox and Müller (6) and Yang et al. (8) but was in contrast to other previous studies showing upper or middle lung predominance mimicking tuberculosis (5, 10) or no lobar predilection (4, 9).

Cavitation and air-filled bronchograms within nodules or consolidation, observed in 58.3% of our cases, have been variably demonstrated in previous studies, ranging from 0% to 42% of cases (4–11, 15). Nonenhanced, low-attenuation areas within the areas of consolidation or masses, previously shown to represent gelatinous collections of large numbers of fungal organisms or rarely ischemic necrosis (12, 15, 16) were also frequently demonstrated on CT images in our study but have rarely been described (17). Calcification within the pulmonary lesion, as shown in one of our cases, is also rare (14, 15, 17, 18). Surrounding groundglass opacity or the CT halo sign, as found in our study, and isolated groundglass opacity (6, 8–11, 17) can be observed. Although centrilobular or satellite nodules have been described (6, 8), tree-in-bud appearance was observed neither in the present nor in previous studies (6–9). Therefore, we suggest that the presence of nonenhanced low-attenuation areas within the areas of consolidation or mass having peripheral, subpleural and lower lung predominance, as shown in the present study, should raise the concern for pulmonary cryptococcosis, particularly in a patient presenting with meningitis.

Endobronchial obstruction in association with other pulmonary abnormalities, similar to our cases, have been described (14, 19), and, unexpectedly, appeared to be more common in immunocompetent patients (19). However, the incidence of direct airway involvement remains unknown (19).

Of interest, more than half of our cases had extrapulmonary findings, including lymphadenopathy, vascular compression, and pericardial or pleural involvement, at the initial presentation. Although lymphadenopathy can be found on CT (5, 6, 8) and can occur in up to two-thirds of immunocompetent patients presenting with cryptococcal pneumonia (15), massive lymphadenopathy causing vascular compression, similar to that in one of our patients, has been reported in only one case in the Korean literature (20). Calcifications of the lymph nodes (14, 15, 17) and/or intracerebral lesions, as found in two of our patients at the initial presentation and after antifungal therapy, are also unusual (21). However, it should be noted that cryptococcosis and tuberculosis might coexist, as presented in one of our cases and in the recent study of Huang et al. (22). Therefore, it might be impossible to exclude other coexisting infections, particularly in the tuberculosis endemic region (22).

Pericardial involvement, as demonstrated in one of our cases, is rarely demonstrated in immunocompetent or immunocompromised hosts (12, 13, 23). As with previous studies, pleural effusion is also uncommon, found in less than 10% of cases, and is often small in size (3–10, 18).

Because *C. neoformans* had been isolated from soils in various parts of Thailand (24), patients who had been working in agriculture or construction fields might have been exposed to a potentially large amount of the fungus, a finding that might explain the relatively extensive disease among Thai patients (12, 13). Different from previous studies in which *C. gattii* occurs mainly in immunocompetent patients in subtropical or tropical countries (1, 6, 25), *C. neoformans var. grubii* (serotype A) was found to be the major organism in the present study, most likely due to a higher prevalence of this variety in Thailand (26). Nevertheless, greater outdoor exposure in men and suppression of the *in vitro* growth of *C. neoformans* by estrogens might explain the male predilection observed in our study and in most of the previous studies (2, 6, 8, 9) and might explain the sporadic case reports from Thailand (12–14).

The presence of poorly formed granulomas in approximately half of our patients, instead of well-formed granulomas with epithelioid or multinucleated giant cells typically found in immunocompetent hosts (6, 16), might reflect the difference or minor functional defect in the host's immune response (27), posing a risk for extensive disease or dissemination in an apparently immunocompetent patient. Therefore, we speculated that the variation in the amount of fungal exposure (3, 12, 15–18), the differences in *Cryptococcal* varieties and their virulence factors in different geographic regions (1, 2, 6, 26), and the variation of an individual host's immune response (2, 16, 27) might influence the difference in clinical features and course of the infection among our patients. However, incomplete data on *Cryptococcal* species or serotypes, histopathological findings, and immunological studies in the present and previous studies precluded further analysis. The issues regarding the effect of *Cryptococcal* varieties on clinical and radiologic features and the risk of extrapulmonary dissemination need further determination.

Following antifungal therapy, we found variable radiologic resolution within the first six months, and substantial improvement (>75%) was usually evident after 12 months of treatment, compared with the more rapid clinical response. As demonstrated in the current and a few recent studies (3, 9, 11), it should be noted that the incomplete and/or gradual radiologic resolution with some residual abnormalities and/or fibrotic scars was a frequent observation among the nonsurgical cases. We speculated that the presence of granulomatous inflammation with fibrosis or a fibrocaseous center demonstrated in the current study and in previous studies (3, 6, 10, 12, 16, 17) should be attributed to a slow regression and incomplete resolution of the radiologic abnormalities and to the development of fibrotic changes, similar to those found in tuberculosis (28). Interval development of cavitation, air bronchograms and/or bronchiectatic changes within the resolving lesions, found in the present study and in

previous studies (6), might be due to dislodgement or drainage of necrotic lung parenchyma and/or gelatinous collection of the fungal organisms. Check-valve bronchiolar obstruction or diffuse pulmonary fibrosis may lead to thin-walled cysts or pneumatocele formation (29, 30) as demonstrated in one of our patients.

As demonstrated in the current study and in previous studies (3, 9, 11), complete radiologic resolution can be achieved only after surgical resection. In an operable case with isolated or persistent pulmonary involvement, particularly in cases with an uncertain diagnosis, surgical intervention may be justified to obviate the need for long-term antifungal treatment (11, 25). Nevertheless, the specific treatment and optimal duration of antifungal therapy for pulmonary cryptococcosis in immunocompetent patients are beyond the scope of our study.

The main limitation in our study was the small number of patients. However, this emphasized the rare occurrence of pulmonary cryptococcosis among immunocompetent patients. Its retrospective nature was another important limitation. Therefore, the initial radiologic images, including the CT technique, as well as types and the timeline of follow-up imaging studies were incomplete and were quite variable among our cases. Nonetheless, our study still provided some useful information that should aid in the diagnosis, treatment, and follow-up of the specific disease entity.

In conclusion, we observed a wide range of clinical and radiologic manifestations, ranging from asymptomatic colonization to disseminated infection, of pulmonary cryptococcosis among Thai immunocompetent patients. Atypical and/or aggressive pulmonary and extrapulmonary involvement, mimicking other more common diseases, was also common. Our findings were different from those reported from other geographic regions; thus, both radiologists and clinicians should be aware of these possibilities. Although the radiologic findings are not specific, the presence of nonenhanced low-attenuation areas within the areas of consolidation or mass with peripheral, subpleural and lower lung predominance and the lack of tree-in-bud appearance on CT should raise concern for pulmonary cryptococcosis, particularly in a patient presenting with meningitis. Importantly, the radiologic resolution of pulmonary cryptococcosis following antifungal therapy was usually gradual and incomplete. Some residual abnormalities, including bronchiectasis, cavitation and/or fibrotic scars, were frequently observed, most notably on CT. Based on our experiences, chest CT may play a role in the diagnostic evaluation and follow-up of severe cases with atypical or aggressive radiologic findings and those requiring long-term antifungal treatment.

Conflict of interest disclosure

The authors declared no conflicts of interest.

References

1. Willenburg KS, Hadley S. Pulmonary cryptococcosis: a rare but emerging disease. Curr Fungal Infect Rep 2009; 3:40–44.
2. Peachey PR, Gubbins PO, Martin RE. The association between cryptococcal variety and immunocompetent and immunocompromised hosts. Pharmacotherapy 1998; 18:255–264.
3. Núñez M, Peacock JE Jr, Chin R Jr. Pulmonary cryptococcosis in the immunocompetent host. Therapy with oral fluconazole: a report of four cases and a review of the literature. Chest 2000; 118:527–534.
4. Nadrous HF, Antonios VS, Terrell CL, Ryu JH. Pulmonary cryptococcosis in nonimmunocompromised patients. Chest 2003; 124:2143–2147.
5. Lindell RM, Hartman TE, Nadrous HF, Ryu JH. Pulmonary cryptococcosis: CT findings in immunocompetent patients. Radiology 2005; 236:326–331.
6. Fox DL, Müller NL. Pulmonary cryptococcosis in immunocompetent patients: CT findings in 12 patients. AJR Am J Roentgenol 2005; 185:622–626.
7. Murayama S, Sakai S, Soeda H, et al. Pulmonary cryptococcosis in immunocompetent patients: HRCT characteristics. Clin Imaging 2004; 28:191–195.
8. Yang CJ, Hwang JJ, Wang TH, et al. Clinical and radiographic presentations of pulmonary cryptococcosis in immunocompetent patients. Scand J Infect Dis 2006; 38:788–793.
9. Chang WC, Tzao C, Hsu HH, et al. Pulmonary cryptococcosis: comparison of clinical and radiographic characteristics in immunocompetent and immunocompromised patients. Chest 2006; 129:333–340.
10. Choe YH, Moon H, Park SJ, et al. Pulmonary cryptococcosis in asymptomatic immunocompetent hosts. Scand J Infect Dis 2009; 41:602–607.
11. Song KD, Lee KS, Chung MP, et al. Pulmonary cryptococcosis: imaging findings in 23 non-AIDS patients. Korean J Radiol 2010; 11:407–416.
12. Areechon W, Prapaiwongs T. Pulmonary cryptococcosis: a case report with lung resection. J Med Assoc Thai 1963; 46:18–23.
13. Prathnadi P, Jiamsripong K, Sorasuchart S, Tantajamroon T, Narco S, Kattipathanapong W. Surgical resection of pulmonary cryptococcosis: report of two cases. Thai J Tuberc Chest Dis 1987; 8:131–135.
14. Piyavisetpat N, Chaowanapanja P. Radiographic manifestations of pulmonary cryptococcosis. J Med Assoc Thai 2005; 88:1674–1679.
15. Feigin DS. Pulmonary cryptococcosis: radiologic-pathologic correlates of its three forms. AJR Am J Roentgenol 1983; 141:1262–1272.
16. Shibuya K, Hirata A, Omuta J, et al. Granuloma and cryptococcosis. J Infect Chemother 2005; 11:115–122.
17. Zinck SE, Leung AN, Frost M, Berry GJ, Müller NL. Pulmonary cryptococcosis: CT and pathologic findings. Comput Assist Tomogr 2002; 26:330–334.
18. Woodring JH, Ciporkin G, Lee C, Worm B, Woolley S. Pulmonary cryptococcosis. Semin Roentgenol 1996; 31:67–75.
19. Karnak D, Avery RK, Gildea TR, Sahoo D, Mehta AC. Endobronchial fungal disease: an under-recognized entity. Respiration 2007; 74:88–104.
20. Hyun JJ, Choi JH, Park S, et al. A case report on cryptococcal lymphadenitis in an immunocompetent adult patient. Infect Chemother 2005; 37:350–354.
21. Berkefeld J, Enzensberger W, Lanfermann H. Cryptococcus meningoencephalitis in AIDS: parenchymal and meningeal forms. Neuroradiology 1999; 41:129–133.
22. Huang CT, Tsai YJ, Fan JY, Ku SC, Yu CJ. Cryptococcosis and tuberculosis co-infection at a university hospital in Taiwan, 1993-2006. Infection 2010; 38:373–379.
23. Levy PY, Habib G, Reynaud-Gaubert M, Raoult D, Rolain JM. Pericardial effusion due to Cryptococcus neoformans in a patient with cystic fibrosis following lung transplantation. Int J Infect Dis 2008; 12:452.

24. Taylor RL, Duangmani C. Occurrence of Cryptococcus neoformans in Thailand. Am J Epidemiol 1968; 87:318–322.
25. Perfect JR, Dismukes WE, Dromer F, et al. Clinical practice guidelines for the management of cryptococcal disease: 2010 update by the infectious diseases society of America. Clin Infect Dis 2010; 50:291–322.
26. Poonwan N, Mikami Y, Poosuwan S, et al. Serotyping of Cryptococcus neoformans strains isolated from clinical specimens in Thailand and their susceptibility to various antifungal agents. Eur J Epidemiol 1997; 3:335–340.
27. Marroni M, Pericolini E, Cenci E, Bistoni F, Vecchiarelli A. Functional defect of natural immune system in an apparent immunocompetent patient with pulmonary cryptococcosis. J Infect 2007; 54:e5–8.
28. Roy M, Ellis S. Radiologic diagnosis and follow-up of pulmonary tuberculosis. Postgrad Med J 2010; 86:663–674.
29. Quigley MJ, Fraser RS. Pulmonary pneumatocele: pathology and pathogenesis. AJR Am J Roentgenol 1988; 150:1275–1277.
30. Shibuya Y, Kitamura S, Sohara Y, Saitoh K. A case of primary pulmonary cryptococcosis associated with pneumothorax. Nihon Kyobu Shikkan Gakkai Zasshi 1995; 33:548–552.